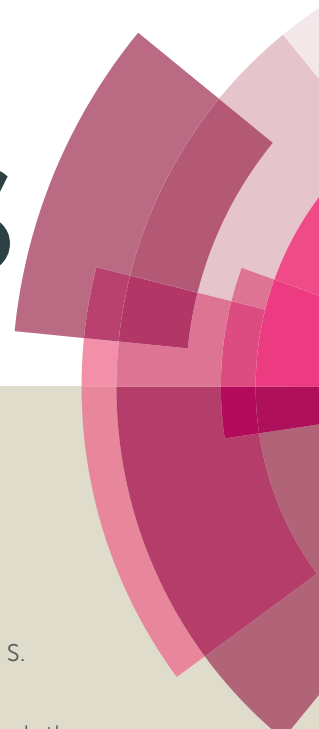


RSC Advances



This article can be cited before page numbers have been issued, to do this please use: P. Maneechakr, S. Karnjanakom and J. Samerjit, *RSC Adv.*, 2016, DOI: 10.1039/C6RA13260J.



This is an *Accepted Manuscript*, which has been through the Royal Society of Chemistry peer review process and has been accepted for publication.

Accepted Manuscripts are published online shortly after acceptance, before technical editing, formatting and proof reading. Using this free service, authors can make their results available to the community, in citable form, before we publish the edited article. This *Accepted Manuscript* will be replaced by the edited, formatted and paginated article as soon as this is available.

You can find more information about *Accepted Manuscripts* in the [Information for Authors](#).

Please note that technical editing may introduce minor changes to the text and/or graphics, which may alter content. The journal's standard [Terms & Conditions](#) and the [Ethical guidelines](#) still apply. In no event shall the Royal Society of Chemistry be held responsible for any errors or omissions in this *Accepted Manuscript* or any consequences arising from the use of any information it contains.

**A facile synthesis of ZnO particles via benzene-assisted co-solvothermal
method with different alcohols and its application**

View Article Online
DOI: 10.1039/C6RA13260J

Panya Maneechakr*, Surachai Karnjanakom and Jittima Samerjit*

*Department of Chemistry, Faculty of Science, Rangsit University, Pathumthani 12000,
Thailand*

*Corresponding author

E-mail: panya.m@rsc.ac.th; samerjit.j@gmail.com

ABSTRACTView Article Online
DOI: 10.1039/C6RA13260J

In this study, ZnO particles with different morphologies are synthesized by a novel solvothermal method with benzene assistance. The prepared samples were characterized by Brunauer–Emmett–Teller (BET) measurement, X-ray diffractometer (XRD), scanning electron microscope coupled with an energy dispersive X-ray detector (SEM-EDX), High-resolution transmission electron microscope (HRTEM), X-ray photoelectron spectrometer (XPS) and H₂-Temperature programmed reduction (H₂-TPR). The results found that the molecular sizes with carbon numbers of alcohols and addition of benzene had great effect on the morphologies, textural properties and crystalline structures of material products in our reaction system. The different ZnO morphologies such as spherical coral-like structure, carnation-like structure, rose-like structure and plate-like structure were obtained using methanol, ethanol, propanol and butanol, respectively. Moreover, Cu particles loaded on ZnO with different morphologies were also investigated for hydrogenation of CO₂ to CH₃OH. The high catalytic activity with selectivity (82.8%) for CH₃OH formation was obtained using ZnO prepared from methanol with Cu doping (Cu/ZnO-Me).

Key words: ZnO; Solvothermal method; Alcohol; Morphology; Hydrogenation

1. Introduction

Nowadays, semiconducting materials with controllable morphologies are more attracted for applications in the industries as well as daily life such as dye-sensitized solar cells, optoelectronic devices, adsorbents, photocatalysis and biosensors.¹⁻⁷ A large number of semiconducting materials such as TiO₂, ZnO and CdS have been identified.⁸⁻¹⁰ Among them, ZnO is considered as one of most promising material due to its non-toxicity, low cost and high catalytic activity, leading to widely practical applications.^{11,12} However, it is still necessary to find the new structures of this material for more appropriate applications. Hence, the development of ZnO material is highly desired and remains a big challenge. Many methods synthesis for synthesis of ZnO have been widely investigated such as hydrothermal, thermal evaporation, sol-gel methods.¹³⁻¹⁵ Nevertheless, synthesis route has some disadvantages, for instance, impurities of ZnO phases are usually found when template was utilized to modify the ZnO structure. To date, no report or any guidance on synthesis, formation mechanism and special morphology of ZnO structure as well as its evolution in a facile benzene-assisted co-solvothermal method using different alcohols can be observed. From stated before, it is an interesting for investigating of this novel method.

As well-known that CO₂ is a main reason on global warming problem as becoming more and more serious in recent years because of the increase of the concentration of CO₂ in air atmosphere. To solve this problem, the use of hydrogenation for conversion of CO₂ to CH₃OH over Cu/ZnO catalysts is an interesting method in the present. Recently, it reported that different ZnO morphologies had a significant effect on its interaction with Cu in the hydrogenation of CO₂ to CH₃OH.¹⁶ They also found that a strong interaction between Cu with ZnO has good selectivity of methanol from CO₂ hydrogenation.

In this work, synthesis of ZnO particles by a facile template-free co-solvothermal method using different alcohols, i.e., methanol, ethanol, propanol and butanol, were studied with assistance of benzene in order to control the morphological structures by just tuning the concentration of benzene. The properties of as-prepared ZnO such as morphology, textural properties and crystalline structure were characterized. The possible synergistic mechanisms of organic solvents on ZnO formation were revealed. The Cu/ZnO catalyst was also applied for hydrogenation of CO₂ to CH₃OH.

2. Experimental

2.1 Preparation of ZnO materials

All reagents were of analytical grade, purchased from Sigma-Aldrich, and used as received without further purification. In a typical synthesis, 5 g of Zn(NO₃)₂·6H₂O was dissolved in 25 ml of methanol (0.60 mol) under vigorous stirring at room temperature until obtained clear solution. Then, 25 ml of benzene as a co-solvent or directing agent was added into the solution with continuously stirred for 10 min, and followed by adding 2.4 g of urea for adjusting pH = 10 and precipitation during reaction process. After complete dissolution, the mixture solution was transferred into a Teflon-lined stainless autoclave and heated at 120 °C for 24 h under the solvothermal process. After cooling down to room temperature, the white solid product was collected by filtration and washed with deionized water for several times, and finally dried in the oven at 80 °C for 12 h. Finally, the ZnO product was stabilized by calcination at 200 °C for 4 h and kept in a desiccator for further characterization and hydrogenation application. Comparing the use of different alcohols, ZnO products were synthesized by using ethanol (0.42 mol), propanol (0.32 mol) and butanol (0.27 mol) as solvents instead of methanol, respectively. The ZnO products were labels as Me, Et, Pr and Bu

corresponding to methanol, ethanol, propanol and butanol, respectively. For Cu/ZnO sample, 1 wt.% of Cu was doped on the prepared ZnO sample by impregnation method. Firstly, a certain amount of prepared ZnO sample was added into the $\text{Cu}(\text{NO}_3)_2 \cdot 3\text{H}_2\text{O}$ solution and stirred at 35 °C for 6 h. Then, the resulting suspension solution was gently dried by heat at 90 °C. The obtained solid product was calcined at 500 °C for 6 h.

2.2 Characterization of ZnO materials

The X-ray powder diffraction (XRD) patterns and the crystallite sizes of samples were determined by using X-ray diffraction (Bruker D8 Advance AXS X-ray Diffractometer) with $\text{CuK}\alpha$ radiation $\lambda = 1.5406 \text{ \AA}$ in the 2θ scan range of 20-70°. The morphologies of samples were investigated by the scanning electron microscope (SEM S-4800; Hitachi) equipped with an X-ray spectrometer for energy dispersive spectroscopy (EDS) analysis. High-resolution transmission electron microscopy (HRTEM) images were obtained from a Philips CM200, model JEOL JEM-2100 transmission electron microscope working at an accelerating voltage of 200 kV. Before HRTEM observation, the sample was dispersed at first in ethanol under ultra-sonication and then dropped on a carbon-coated copper grid, which was dried at room temperature. The specific surface areas of samples were obtained from N_2 adsorption and desorption isotherms using a Quantachrome Autosorb 1 gas adsorption analyzer at -196 °C. All the samples were degassed at 150 °C in vacuum for 2 h prior to measurements. The surface areas were calculated from Brunauer–Emmett–Teller (BET) method, and the pore size and pore volume were determined by the Barrett–Joyner–Halenda (BJH) method from desorption branch of the isotherms. X-ray photoelectron spectroscopy (XPS) measurement was analyzed on a PerkinElmer PHI 5000C system with a $\text{Mg K}\alpha$ X-ray source ($h\nu = 1253.6 \text{ eV}$). The reduction behaviour of Cu/ZnO sample was performed

using H₂-Temperature-programmed reduction (TPR) with a gas mixture of 5 vol% H₂ in N₂ at a flow rate of 50 ml/min. View Article Online
DOI: 10.1039/C6RA13260J

2.3 Catalytic evaluation

Catalytic activity of as-prepared sample was evaluated using a fix-bed reactor. In short, 0.1 g of catalyst diluted with quartz sand was loaded into the quartz tube. Before catalytic test, catalysts were reduced with H₂ flow (flow rate = 50 ml/min) at 350 °C for 1 h under atmospheric pressure. Then, the reactor was cooled to 180 °C and the reactant gas flow was introduced. The reaction conditions fixed for all experiments were 240 °C, 3 MPa, 0.54 mol/(g_{-cat} h) and molar feed composition of H₂/CO₂ = 3/1. The products were analyzed online by a gas chromatograph equipped with a thermal conductivity detector.

3. Results and discussion

Fig. 1a shows the XRD pattern of as-synthesized products. As revealed, the typical diffraction peaks at 31.8, 34.6, 36.3, 47.7, 56.7, 62.9, 66.6, 68.1 and 69.2° are attributed to the (100), (002), (101), (102), (110), (103), (200), (112) and (201) crystal planes, respectively.¹⁷ No other crystalline impurities of ZnO structure are detected in the XRD pattern, indicating that high phase purity of ZnO structure is obtained in our method. In order to investigate the crystallite size of each product, the Scherrer's equation (ep.1), is applied for the calculation as follows:

$$D = \frac{K\lambda}{\beta \cos(\theta)} \quad (1)$$

Where K is the Scherer constant (K=0.89), λ is X-ray radiation wavelength ($\lambda = 1.5406 \text{ \AA}$), θ the Bragg's angle at which the peak is observed measured in radians, and β is the full width of diffraction line at half of the maximum intensity (FWHM).¹⁸ The average crystallite size of

the samples are calculated and listed in Table 1. One can see that ZnO crystallite size increases when the carbon number or molecular sizes in the alcohols increases, suggesting that the alcohol with longer alkyl chain based on the relative of carbon number is favorable for the formation of ZnO with higher crystallinity. It should be noted that different kinds of alcohols are utilized as a solvent in an equal volume but moles of alcohol molecules are different in the system, i.e., methanol > ethanol > propanol > butanol. In this case, during the reactions, smaller alcohol molecule size can be intercalated the Zn(OH)₂ layer structures more easily as large amounts of alcohol molecules show the better growth and arrangement of ZnO unit cells.¹⁹ As stated above, even the molecular size has a great effect but polarity of alcohol is also a main important factor. The stronger polarity is favorable for making the hydrogen bonds between alcohol molecules with hydroxides surface, for instance, the methanol has strongest polarity which improves the CH₃-O groups combination or adsorption with the surface hydroxyl groups of ZnO crystallites.¹⁹ As expected, the ZnO-Me exhibits a relatively lower crystallinity than others. In addition, it reveals that nitrate groups derived from zinc compound could affect to adsorb on product surface, resulting in the different crystallite formation as well as morphologies with pore structures.²⁰ However, an increase of carbon number results larger molecular size of alcohol, which could lead to that nitrate groups adsorbing on product surface becomes more and more difficult due to effects of polarity and steric. Further evidence of the formation of ZnO with high purity is the EDX analysis. The Zn and O peaks can be clearly observed in Fig 1b. It should be mentioned here that C peak was also detected which obtained from the supporting carbon tape (Fig. 1b).

Fig. 2 shows the SEM images of as-synthesized products. As observed, different morphologies of ZnO structures are obviously obtained when the different types of alcohols are used. Fig. 2a shows SEM image of ZnO-Me with spherical coral-like structure. When ethanol is used to replace of methanol, carnation-like structure is formed (Fig. 2b) When

propanol and butanol are applied, rose-like structure and plate-like structure are obtained, respectively (Fig. 2c and d). From these results, the different alcohols have a great effect on formation of ZnO structures. In the initial stage of reaction, $\text{Zn}(\text{NO}_3)_2 \cdot 6\text{H}_2\text{O}$ is dissolved into different alcohols and then formed metastable zinc alkoxide ($\text{Zn}(\text{OH})_m(\text{OR})_n$). As the reaction proceeded, the condensation between ($\text{Zn}(\text{OH})_m(\text{OR})_n$) molecules took place and $\text{Zn}(\text{OH})_x$ crystallites are formed.²¹ Due to large amounts of OH groups on the surface of these crystallites and alcohol molecules existing in the system, the -OR groups may readily bond to the surface of $\text{Zn}(\text{OH})_x$ crystallites through H bonds and electrostatic force, while alkyl chains head away from the surface. In case of ZnO-Me, due to methanol molecules possess small steric bulkiness, the corresponding crystallites could self-assemble into tight spherical particles. For ZnO-Et, ZnO-Pr and Zn-Bu, their crystallites bonding formed into loose plate shapes. HRTEM images of samples was also observed as can be seen in Fig. 2a-d. The results exhibit lattice fringes of the ZnO crystal, which corresponds to the (002) plane of ZnO. It should be concluded here that the certain morphologies in each sample can be obtained by assistance of benzene. In this work, volume ratio of alcohol to benzene (25 ml to 25 ml) is an optimum condition to obtain the certain ZnO structure in our preliminary experiments. When volume ratio volume ratios of propanol to benzene are changed, irregular and non-uniform of ZnO structures are clearly observed (Fig. 2). In this study, ZnO-Pr was selected as an example for investigation on the change of ZnO morphology when benzene amount is adjusted. Fig. 2e-h show the SEM images of product obtained from using different volume ratio of propanol to benzene. When amount of benzene is added an increase or a decrease in the system from optimum value (25 ml), irregular shape of ZnO-Pr can be observed. It demonstrates that benzene has a great influence on the morphology of products. Here, it is possible that benzene bears quite weak polarity and dissolubility in contrast with alcohol, but both of them affected the hydrolyzation of Zn-alcoholic complex and the

View Article Online
DOI: 10.1039/C6RA13260J

formation of products. When the benzene is added in optimum amount, the benzene molecules could be adsorbed on the surface of amorphous $\text{Zn}(\text{NO}_3)_2$ particles by physicochemical reaction process, leading to the decrease in the surface free energy of them.²² These behaviors affect to the growth of crystallites along a certain direction to some extent and promote the formation of certain structures. Moreover, in Fig. 3, when ZnO-Pr is calcined at high temperature of 500 °C for 4 h, its morphology can further changed to worm-like structure due to hydration reaction and agglomeration.

Fig. 4 shows the N_2 adsorption-desorption isotherms of ZnO-alcohol products. All products exhibit an International Union of Pure and Applied Chemistry (IUPAC) type IV isotherm with a significant hysteric loop above relative pressures P/P_0 of 0.45, indicating the existence of ink-bottle mesoporous in these materials. The textural properties of ZnO-alcohol products are listed in Table 1. It can be seen that when the carbon number of alcohol increased, the surface area decreased while pore size increased. It is possible that weak crystalline structure has a lot of defects on agglomerated particles (secondary particles), resulting that the larger amount of pores between single-particle without agglomeration (primary particles) and these pores are very small. It is why ZnO-Me has higher surface area even the morphology is tight spherical. In contrast, when the primary crystallites are better crystalline, the corresponding secondary particles have few defects and most pores arise from the packing spaces between secondary particles. Thus, lowest surface area and largest pore size should be ZnO-Bu. Fig. 5 shows XPS patterns of ZnO synthesized by different alcohols. It is found that the binding energy of O 1s for the ZnO-Me (532 eV) is lower than others and become lower and lower when increasing the C number of alcohol for ZnO synthesis, indicating that electrons are easier to be excited from the ZnO-Me and the ZnO-Me has more oxygen vacancies and larger polar planes when comparing with others.²³

In this study, hydrogenation of CO₂ to CH₃OH was also investigated over 1 wt% Cu/ZnO samples. The fix-bed reactor was used for performance evaluation of catalyst. The reaction conditions fixed for all experiments were 240 °C, 3 MPa, 0.54 mol/(g_{cat} h) and molar feed composition of H₂/CO₂ = 3/1. The catalytic activity results of as-prepared catalysts for CO₂ hydrogenation are shown in Fig. 6. One can see that the best catalytic activity for CO₂ hydrogenation to CH₃OH with a 18% conversion of CO₂ and 82.8% selectivity of CH₃OH is obtained using Cu/ZnO-Me. It is probably due to stronger interaction between Cu and ZnO and more amounts of surface oxygen vacancies in Cu/ZnO-Me.²³ In addition, in case of largest surface area of ZnO-Me, Cu should be better well-dispersed than others, resulting in the increasing of active sites. To support the explained assumptions, H₂-TPR and XPS analyses for each catalyst are also investigated and the results are shown in Fig 7. Fig. 7a shows H₂-TPR results for investigating on reduction behavior of Cu/ZnO catalysts. H₂ was feed to CuO on sample with an increasing of temperature. During this process, CuO can be reduced to Cu with an appropriate temperature range based on interaction between metal oxides with supports. It should be mentioned here that all catalysts exhibit reduction profiles as a broad band of H₂ consumption below 350 °C. This indicates that appeared peak has only CuO reduction while ZnO reduction is not found due to its reduction properties generally (>500 °C). The H₂-TPR patterns of all Cu/ZnO samples can be attributed to the two step-reduction of Cu²⁺ to Cu⁺ with Cu⁺ to Cu⁰.²⁴ Interestingly, the reduction temperature of CuO species in Cu/ZnO-Me is higher than others, indicating that Cu prepared on ZnO-Me has strongest interaction and best dispersion. In addition, it can be clearly seen that alcohol has also effect to improve the interaction of ZnO with Cu. Fig 7b shows the XPS patterns of Cu/ZnO catalysts. As expected, binding energy value of Cu 2p_{3/2} of Cu/ZnO-Me is lower than another catalyst, resulting from better electrons transfer and more amount of oxygen

vacancy. This is that why Cu/ZnO-Me has better catalytic activity on hydrogenation of CO₂ to CH₃OH.

View Article Online
DOI: 10.1039/C6RA13260J

4. Conclusions

In summary, based on a facile benzene-assisted solvothermal method with different alcohol from C₁ to C₄, the different ZnO morphologies such as spherical coral-like structure, carnation-like structure, rose-like structure and plate-like structure were obtained. The carbon number, molecular sizes and polarities of alcohols had a great effect on the formation mechanism of ZnO structures. The benzene had a significant synergistic influence with alcohols on the morphology and formation process of ZnO product. Cu/ZnO-Me showed the best catalytic activity for hydrogenation of CO₂ to CH₃OH with high selectivity due to characteristic of its physicochemical properties.

Acknowledgments

The authors wish to acknowledge Department of Chemistry, Faculty of Science, Rangsit University for supporting all instruments and chemicals.

References

- 1 Q. Yang, J. Duan, P. Yang and Q. Tang, *Electrochim. Acta*, 2016, **190**, 648–654.
- 2 C. Zhang, Y. Xie, T. Bai, J. Hu and J. Wang, *J. Power Sources*, 2015, **297**, 16-22.
- 3 D. W. Mohammed, R. Waddingham, A. J. Flewitt, K. A. Sierros, J. Bowen and S. N. Kukureka, *Thin Solid Films*, 2015, **594**, 197–204.
- 4 W. Zhang, L. Meng, G. Mu, M. Zhao, P. Zou and Y. Zhang, *Appl. Surf. Sci.*, 2016, **378**, 196–206.

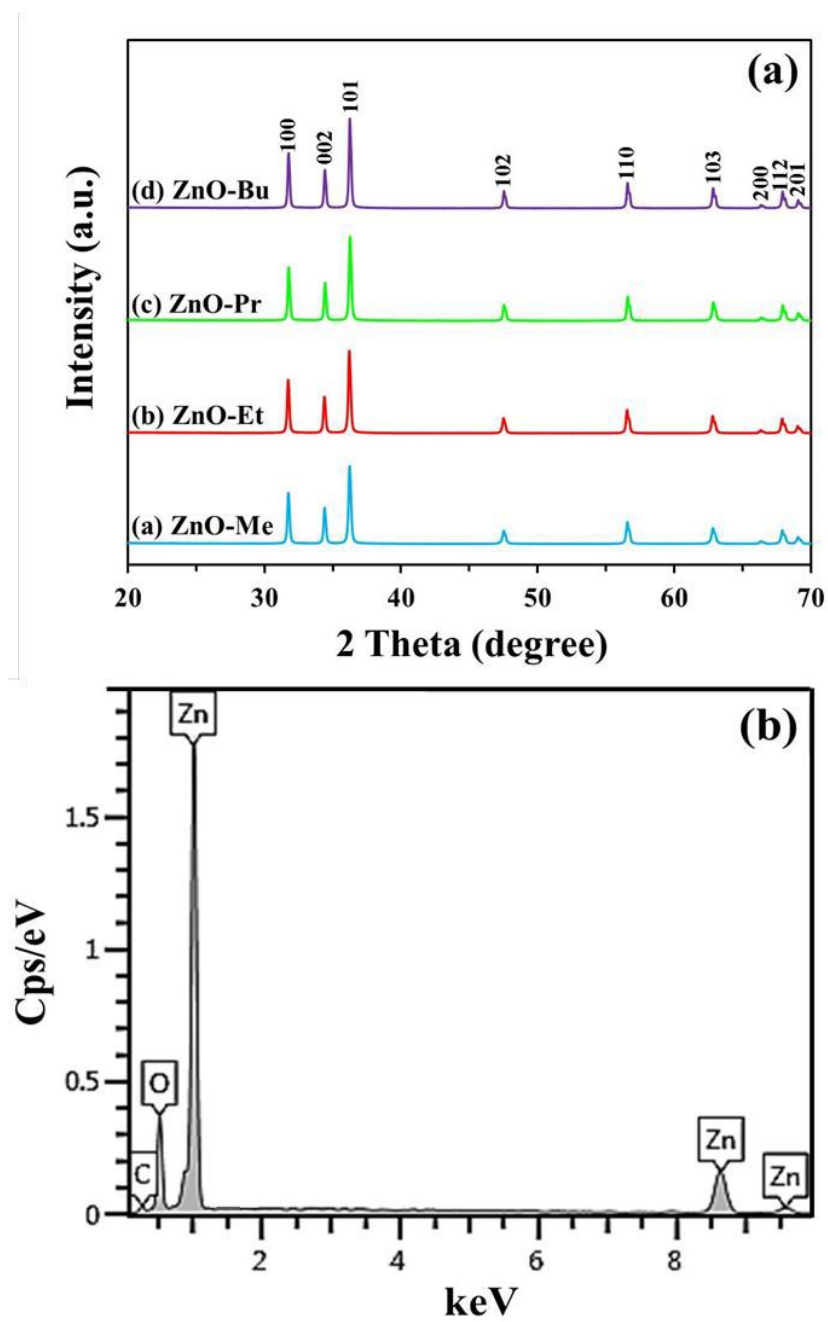
- 5 Q. Li, E. T. Liu, Z. Lu, H. Yang and R. Chen, *Mater. Lett.*, 2014, **130**, 115-119. View Article Online
DOI: 10.1039/C6RA13260J
- 6 A. Sadollahkhani, I. Kazeminezhad, J. Lu, O. Nur, L. Hultman and M. Willander, *RSC Adv.*, 2014, **4**, 36940–36950.
- 7 Y. Zhou, L. Wang, Z. Ye, M. Zhao and J. Huang, *Electrochim. Acta*, 2014, **115**, 277–282
- 8 Y. Chen, C. Zhang, W. Huang, Y. Situ and H. Huang, *Mater. Lett.*, 2015, **141**, 294–297.
- 9 G. Cappelletti, V. Pifferi, S. Mostoni, L. Falciola, C. D. Bari, F. Spadavecchia, D. Meroni, E. Davoli and S. Ardizzone, *Chem. Commun.*, 2015, **51**, 10459-10462.
- 10 F. Vaquero, R. M. Navarro and J. L. G. Fierro, *Int. J. Hydrogen Energy*, 2016, **41**, 11558-11567.
- 11 K. M. Fang, Z. Z. Wang, M. Zhang, A. J. Wang, Z. Y. Meng and J. J. Feng, *J. Colloid Interface Sci.*, 2013, **402**, 68-74.
- 12 P. N. Mbuyisa, O. M. Ndwandwe and C. Cepek, *Thin Solid Films*, 2015, **578**, 7-10.
- 13 P. Ramu, P. M. Anbarasan, R. Ramesh, S. Aravindan, S. Ponnusamy, C. Muthamizhchelvan and Z. Yaakob, *Mater. Lett.*, 2014, **122**, 230-233.
- 14 T. Tian, J. Xing, L. Cheng, L. Zheng, W. Ruan, X. Ruan and G. Li, *Ceram. Int.*, 2015, **41**, S774–S778.
- 15 Y. T. Chung, M. M. Ba-Abbad and A. W. Mohammad, *Mater. Des.*, 2015, **87**, 780-787.
- 16 F. L. Liao, Y. Huang, J. Ge, W. Zheng, K. Tedsree, P. Collier, X. Hong, and S. C. Tsang, *Angew. Chem.*, 2011, **50**, 50, 2162 –2165.
- 17 X. L. Xu, Y. Chen, S. Y. Ma, S. H. Yan, Y. Z. Mao, T. Wang and H. Q. Bian, *Mater. Lett.*, 2015, **151**, 5-8.

- 18 M. Hosni, S. Farhat, F. Schoenstein, F. Karmous, N. Jouini, B. Viana and A. Mgaidi, *J. Alloys Compd.*, 2014, **615**, S472-S475. View Article Online
DOI: 10.1039/C6RA13260J
- 19 D. A. Johnson, R. Shaw, E. F. Silversmit, *J. Chem. Edu.*, 1994, **71**, 517
- 20 G. Li, Y. Liu and C. Liu, *Microporous Mesoporous Mater.*, 2013, **167**, 137-145.
- 21 A. K. Radzimska, T. Jesionowski, *Materials*, 2014, **7**, 2833-2881.
- 22 Z. Tang, J. Liang, X. Li, J. Li, H. Guo, Y. Liu and C. Liu, *J. Solid State Chem.*, 2013, **202**, 305-314.
- 23 F. L. Liao, Y. Q. Huang, J. W. Ge, W. R. Zheng, K. Tedsree, P. Collier, X. Hong and S. C. Tsang, *Angew. Chem.*, 2011, **123**, 2210-2213.
- 24 K. M. Parida and D. Rath, *J. Colloid Interface Sci.*, 2009, **340**, 209-217.

Table captionView Article Online
DOI: 10.1039/C6RA13260J**Table 1** Textural properties of ZnO products synthesized by different alcohols.**Figure captions****Fig. 1** (a) XRD patterns of ZnO products synthesized by different alcohols and (b) EDX spectrum of ZnO product.**Fig. 2** SEM images of (a) ZnO-Me, (b) ZnO-Et, (c) ZnO-Pr, (d) ZnO-Bu and ZnO-Pr products synthesized by different volume ratios of propanol to benzene: (e) 5 to 45, (f) 15 to 35, (g) 25 to 25, (h) 35 to 15 and (i) 45 to 5. HRTEM images were inserted in (a), (b), (c) and (d)**Fig. 3** SEM image of ZnO-Pr (propanol to benzene = 25 to 25) which calcined at 500 °C for 4 h.**Fig. 4** N₂ adsorption-desorption isotherms of ZnO products synthesized by different alcohols.**Fig. 5** XPS patterns of ZnO products synthesized by different alcohols.**Fig. 6** Performance testing of as-prepared catalysts for the hydrogenation of CO₂.**Fig. 7** (a) H₂-TPR profiles and (b) XPS patterns of 1 wt.% Cu loaded ZnO products synthesized by different alcohols.

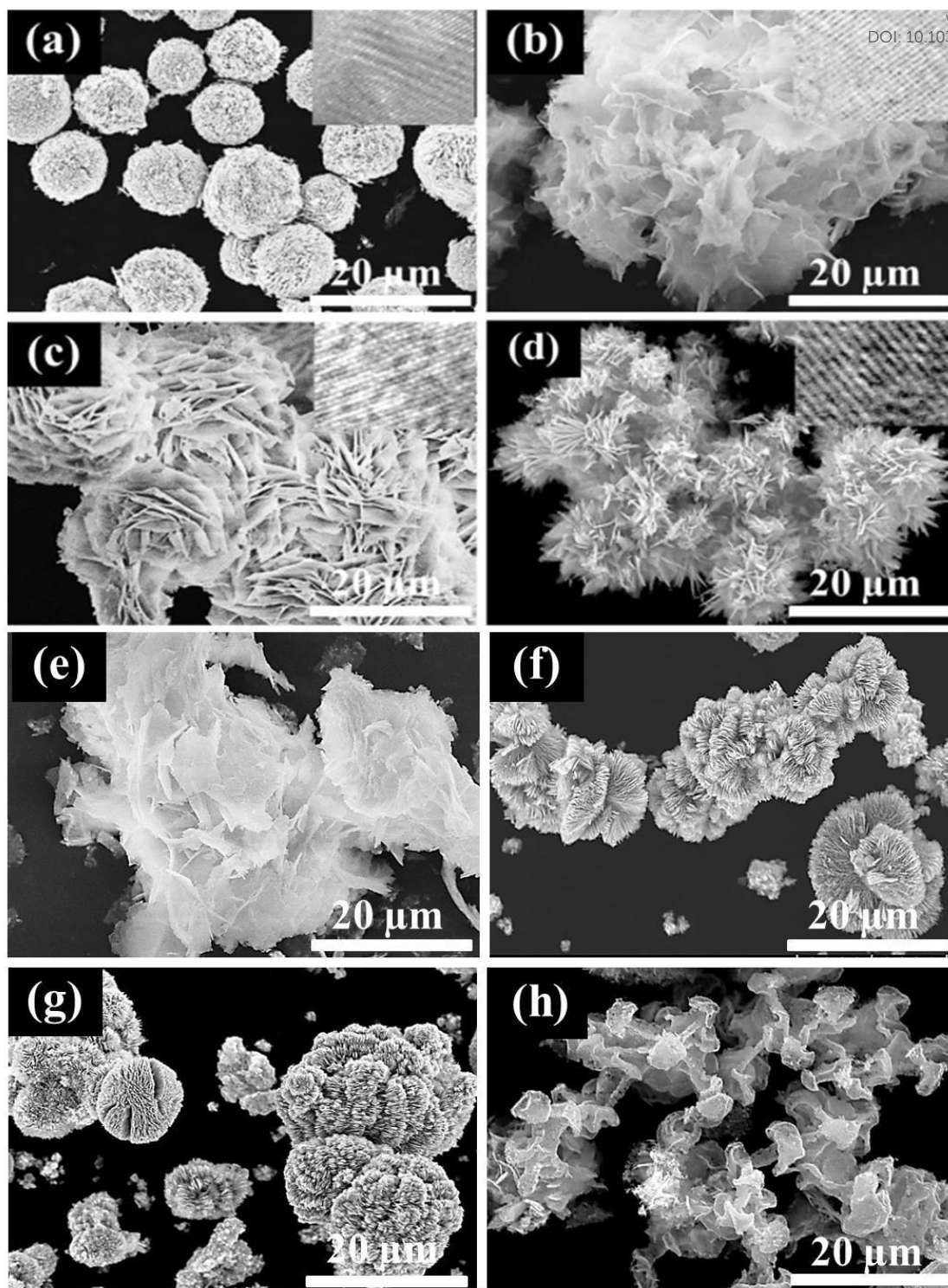
Table 1 Textural properties of ZnO products synthesized by different alcohols.View Article Online
DOI: 10.1039/C6RA13260J

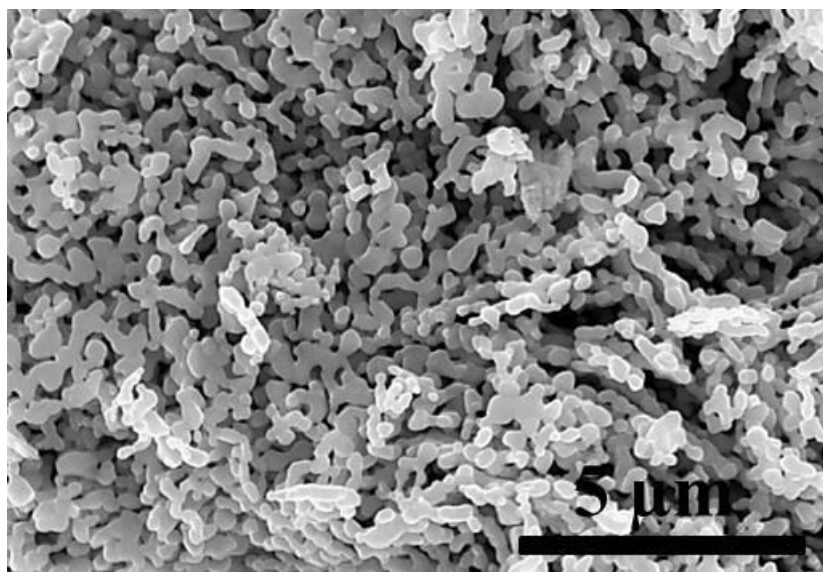
Sample	Surface area (m ² /g)	Pore volume (cm ³ /g)	Pore diameter (nm)	Crystallite size (nm)
ZnO-Me	63.2	0.22	2.3	35.8
ZnO-Et	41.6	0.51	3.4	36.5
ZnO-Pr	37.7	0.87	5.1	37.3
ZnO-Bu	20.9	0.92	6.4	39.9



View Article Online
DOI: 10.1039/C6RA13260J

Fig. 1

**Fig. 2**



View Article Online
DOI: 10.1039/C6RA13260J

Fig. 3

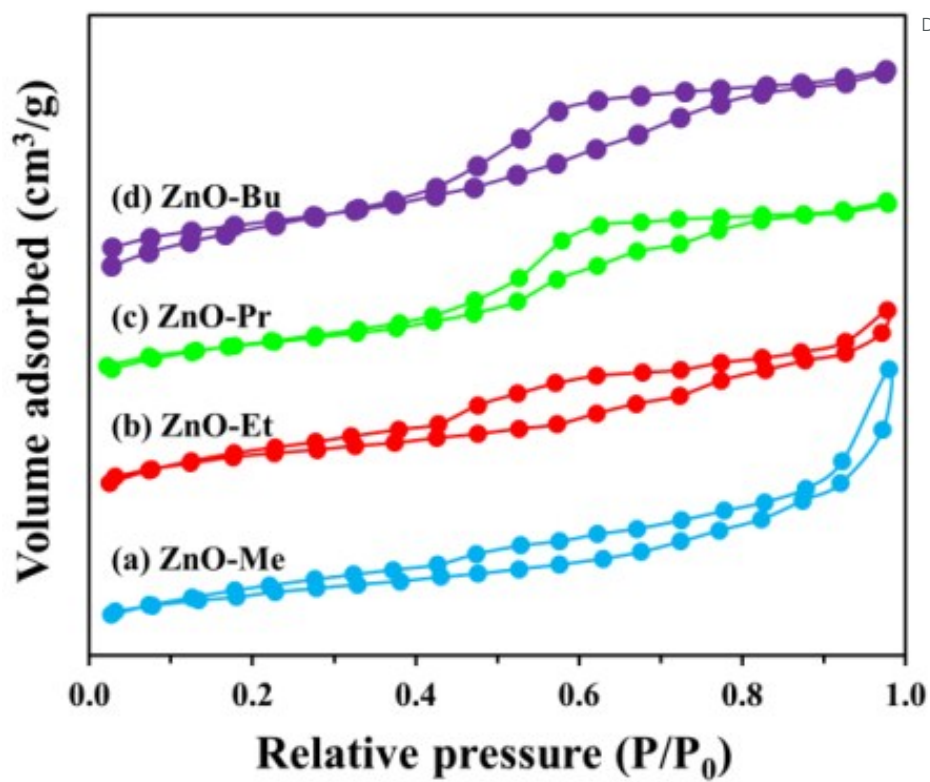


Fig. 4

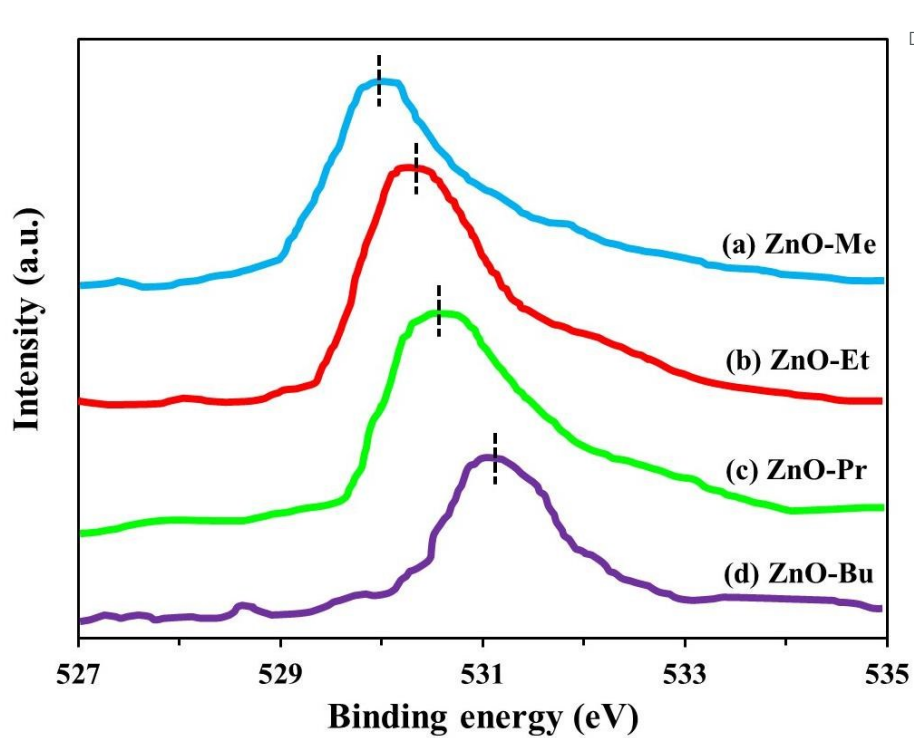


Fig. 5

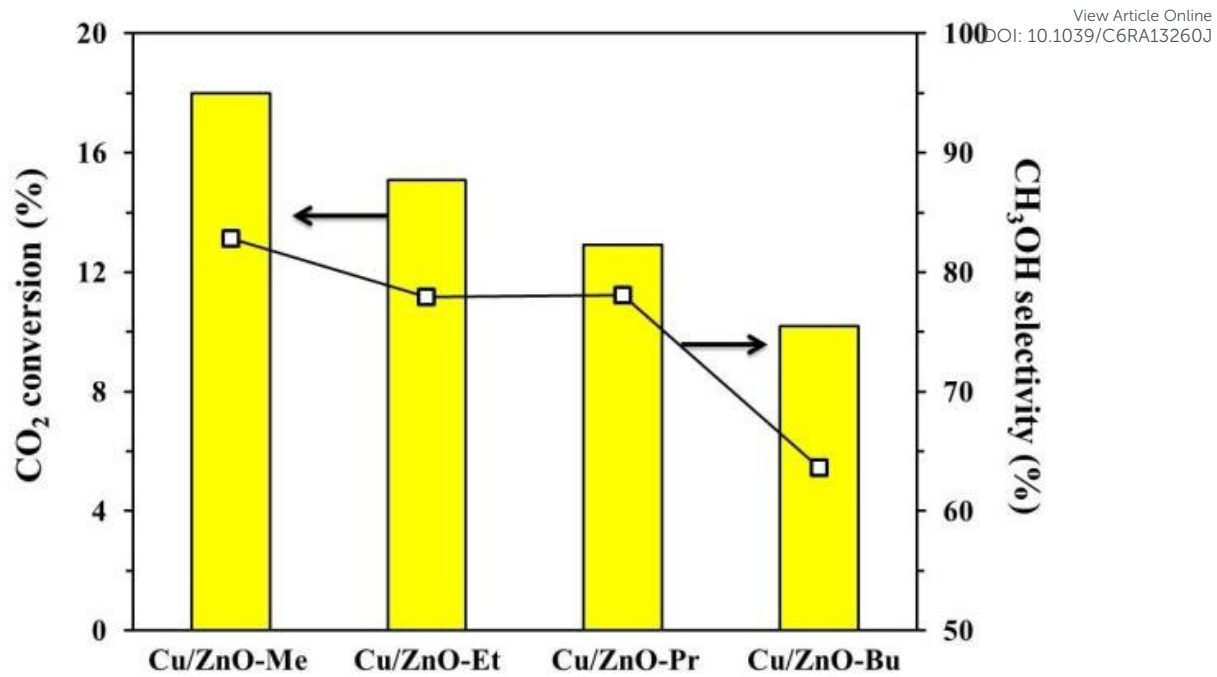


Fig. 6

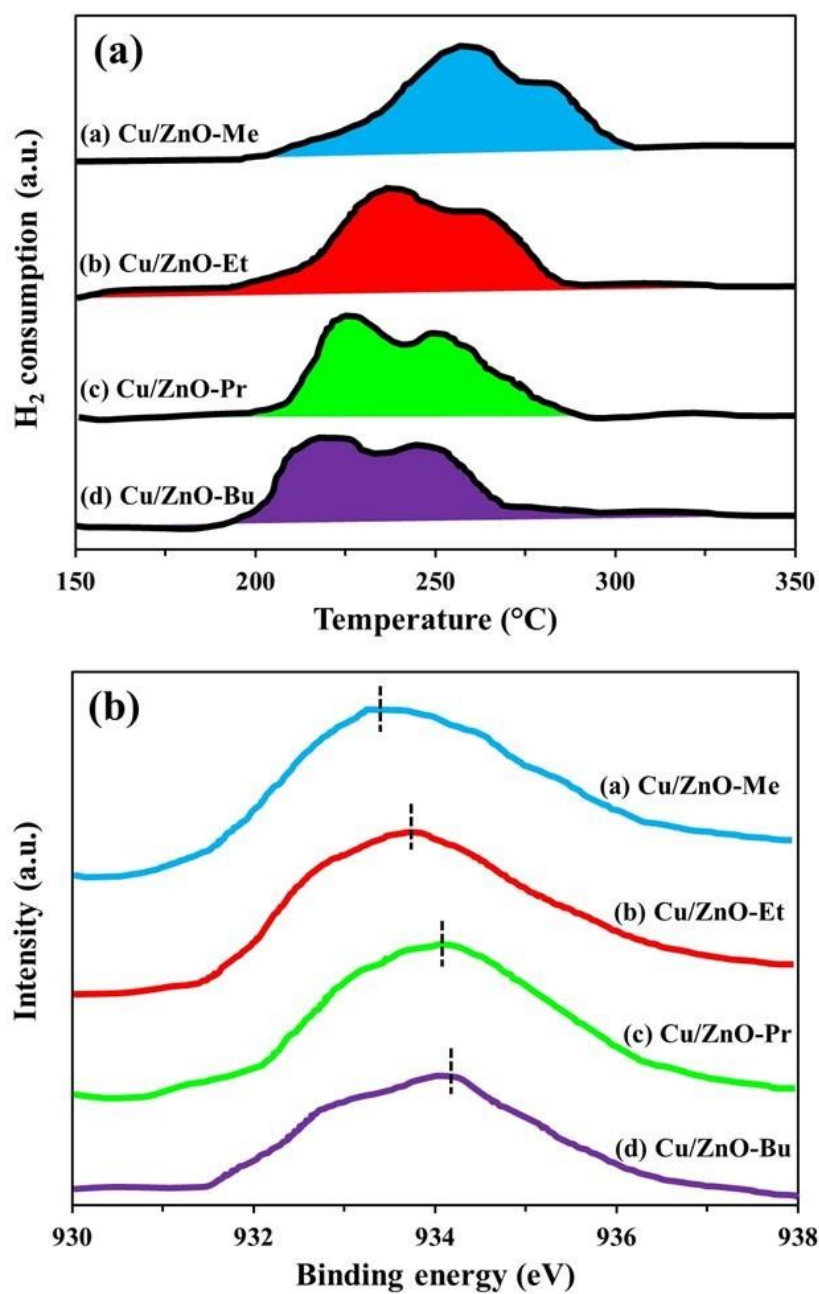


Fig. 7

Table of Contents

